ESTIMATION OF INTERIOR ORIENTATION AND ECCENTRICITY PARAMETERS OF A HYBRID IMAGING AND LASER SCANNING SENSOR

A. Wendt[a], C. Dold[b]

[a]Institute for Applied Photogrammetry and Geoinformatics, University of Applied Sciences Oldenburg, Ofener Straße 16/19, D-26121 Oldenburg, Germany

[a]Institute of Photogrammetry and GeoInformation, University of Hannover, Nienburger Str. 1, D-30167 Hannover, Germany

[b]Institute of Cartography and Geoinformatics, University of Hannover, Appelstr. 9A, D-30167 Hannover, Germany

(a.wendt@fh-oldenburg.de, christoph.dold@ikg.uni-hannover.de)

Commission V, WG V/1

KEY WORDS: Calibration, Terrestrial laser scanning, Hybrid measurement system, Sensor fusion

ABSTRACT:

Nowadays hybrid imaging and laser scanning sensors are common for terrestrial surveying purposes. The basic idea is to complement laser scanning, which directly yields 3D information, with digital image capture, which delivers high resolution images for measurement and texturing. The image sensors are internally built in a scanner or externally mounted on top. The advantage of external mounted devices is the flexibility of the used sensors. Depending on the application, cameras with a different resolution or focal length can be used. Such systems are handy, but the calibration parameters have to be determined or controlled for each sensor and every mount. Hybrid systems offer new possibilities such as monoplotting using a combination of images and 3D point clouds or automatic orientation procedures. Furthermore, the fusion of both data sources will generally lead to a higher accuracy and reliability.

These facts emphasize the importance of an accurate calibration between the single sensors of a hybrid system. The calibration can be subdivided into three tasks, calibration of the scanning system, the imaging sensor and the estimation of the eccentricity between the sensors. While scanning systems are usually calibrated by the manufacturer, the calibration of the imaging sensor and the estimation of the eccentricity have to be done on the job by the user with provided calibration software. These calibration tasks are discussed in detail in this paper.

Based on the fact that the camera is mounted on the scanner, a comparison between single image and multiple image calibration is done regarding to the accuracy. The comparison is realized with a suitable 3D test field, as it is used in close range photogrammetry. The differences of the single image calibration to the multiple image calibration as reference values are given. The single image calibration is about three times worse in inner and outer accuracy. Further mainly for the eccentricity, a three-dimensional test field is created. In a practical test the eccentricity calibration with and without commonly adjusted camera calibration parameters is evaluated. It is emphasized that the eccentricity parameters are highly correlated with the interior orientation parameters. The most reliable result of the eccentricity calibration could be obtained by integrating the interior orientation of the multiple image calibration fixed.

1. INTRODUCTION

1.1 Terrestrial Laser scanning

Terrestrial laser scanners become more and more popular for surveying purposes. There are many different applications where such scanners are used, for example monitoring, documentation of monuments and historic buildings, data acquisition of buildings as a basis for city modeling or indoor measurements in buildings. Terrestrial laser scanners provide a dense three dimensional point cloud of the scanned object. Most scanners work with a similar principle. A laser-light pulse is emitted, parts of it are reflected at an object and received and registered by the instrument. The distance is usually determined from the time of flight of the laser pulse or in some cases by triangulation (close range scanners). Most scanners measure with a high scan rate. The laser beam is deflected by rotating or oscillating mirrors in the vertical direction. The horizontal deflection is usually done by rotating the measurement device of the scanner. Modern scanners cover an area of 360 degrees horizontally and are often termed as panorama scanners for this reason. The vertical field of view is often limited, but some models are able to scan a complete dome (up to 270 degrees). Terrestrial laser scanners are classified by their maximum measurement range. Usually they are divided in three groups: close range, mid range and long range scanners. There are considerable differences in the accuracy of the single measurements and the spot sizes of the laser scanner instruments.

The standard scanning procedure in practice is to position the scanner system and to acquire data from the surrounding area. In order to obtain data of a complete object it is necessary to collect data from various locations. For each position a new local coordinate frame is defined. The multiple frames are usually transformed into one common coordinate frame for data processing.

1.2 Hybrid Sensors

Many scanner systems are equipped with an additional image sensor. The distance measurement unit and the digital camera unit form a hybrid sensor system. Thus, image data and 3D point data can be combined. In general, to each measured 3D point a color value acquired by the camera unit is assigned. Thereby the processing of the laser data is simplified for human operators, because it is easier to relate colored points to objects. For instance Becker et al. (2004) describe a system for processing laser scanning and photogrammetric data simultaneously. Furthermore the images can be used for texturing models or objects, which are derived from the laser scan data.

The manufactures of laser scanners use different techniques for the combination of laser scanners with digital cameras. One method is the integration of a camera in the body of the scanner. In this case scanner and image sensor are combined to one unit. Examples are the GS series from Mensi (Mensi, 2005), Leica (Leica, 2005) with its HDS3000 scanner and Callidus (Callidus, 2005). Another concept used by Riegl for the LMS-Z series (Riegl, 2005) and iQvolution for the iQsun series (iQvolution, 2005) for instance, is to mount a digital camera externally on the top of the scanner. Both techniques have several advantages and disadvantages. The major drawback of externally mounted camera units is the weak calibration of such systems. Since the distance and camera unit are only connected by clamping system and are usually disconnected for transportation, the calibration of the system should be done for each mount. The advantage lies in the flexibility of the used sensors. Depending on the application, cameras with a different resolution or focal length can be used for data acquisition. Thus, the resolution of distance and camera unit may be adapted to each other.

This paper is limited to hybrid sensors with externally mounted camera units. A Riegl LMS-Z360 scanner in combination with Nikon D100 camera was available for measurements. The hybrid system is shown in figure 1.

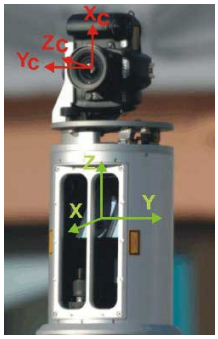

Figure 1: Combined sensor - laser scanner with mounted camera (Riegl, 2005)

We describe the calibration of the interior orientation of the camera unit and the estimation of its eccentricity to the laser scanning sensor. The scanning sensor itself is calibrated by the manufacturer. Firstly, we describe the required calibrations of a hybrid scanner. Also the estimation of the eccentricity parameters between the sensors will be explained. In order to evaluate the quality of the camera calibration in comparison to being mounted on the scanner or not, we compare multi and single image calibration using a close range test field. This is done under ideal conditions in a laboratory test. In a practical test, the eccentricity is calibrated in a laboratory hall. There we have installed a test field with retro-reflected targets. Also the recommended calibration method of the manufacturer to estimate the eccentricity and image calibration simultaneously is done in this test.

Finally, we conclude this work and give some statements to the resulting accuracy of the calibration methods.

2. CALIBRATION METHODS

The full system calibration of a hybrid sensor can be separated into three single calibrations:

a) Calibration of the scanner
b) Calibration of the eccentricity
c) Calibration of the camera

Usually the scanner is calibrated by the manufacture and will not be discussed here. The calibration of the eccentricity in contrast can only be done in combination with the scanner. It will be discussed in detail. Therefore the mathematic model for the estimation is derived. It is shown, that this model could be extended with the unknowns of each single sensor. The calibration of the interior orientation of the camera should be done at the same time of the measurement campaign. It is a standard photogrammetric task in close range applications.

2.1 Calibration of the eccentricity

2.1.1 Relation between camera and laser scanner sensor

As shown in fig. 1, the camera sensor is mounted on top of the laser scanner. The geometric relation between both coordinate frames is given in fig. 2.

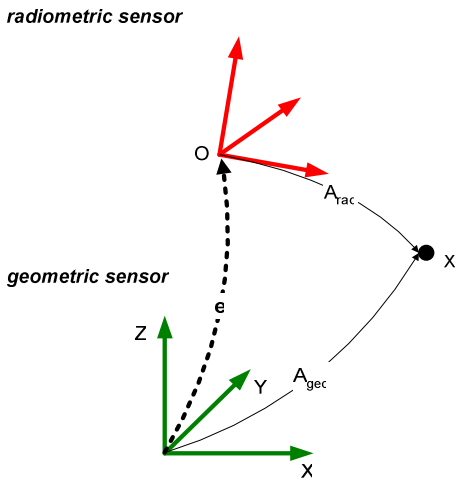

Figure 2: Relation between radiometric (camera) and geometric (laser scanner) sensor

The origin of the coordinate frame of the geometric sensor is defined as a right handed system, the zero direction of the horizontal pitch circle defines the x-axis. The definition of the coordinate system of the geometric sensor is also the definition of the whole hybrid sensor system.

On the other hand the origin of the coordinate frame of the radiometric sensor is the projection centre O'. This coordinate frame is defined by the camera. The orientation of this radiometric coordinate frame within the hybrid sensor system is described by the eccentricity between the sensors (fig. 1).

The goal of the calibration of the eccentricity is the estimation of three rotational and three translational parameters between the two coordinate frames. Thus, the eccentricity includes six degrees of freedom.

However, in fig. 2 is also shown, that the observations of the laser scanner and the images are related to the object space by their mapping functions. In case of the calibration of the eccentricity it is supposed that these functions are completely known. The mapping functions are:

$$X_i = A_{geo}(d, \phi, \theta) \quad (1)$$

$$X_i = A_{rad}(e(T_E, R_E), ior, x', y')) \quad (2)$$

With:

X_i	3D control point in object space
A_{geo}	Geometric mapping function
ϕ, θ	Measured angles of the control point
d	Measured distance to the control point
A_{rad}	Radiometric mapping function
$e(T_E, R_E)$	Eccentricity
ior	Interior orientation of the camera
x', y'	Image coordinates of the control point

2.1.2 Calibration

For the calibration of the eccentricity a complementary aspect of the relation between the sensors has to be introduced. An individual rotation angle of the radiometric sensor around the z-axis of the scanner is a part of the actual relation between the sensors. Fig. 3 demonstrates this connection. The figure shows the top view of the scanner. Each position of the radiometric sensor is observed by the already calibrated scanner. Thus the rotation angle is treated as constant.

By this rotation angle the image frame is related to the x-axis of the geometric sensor. The eccentricity is defined between the sensors when the radiometric sensor is aligned to the x-axis of the geometric sensor.

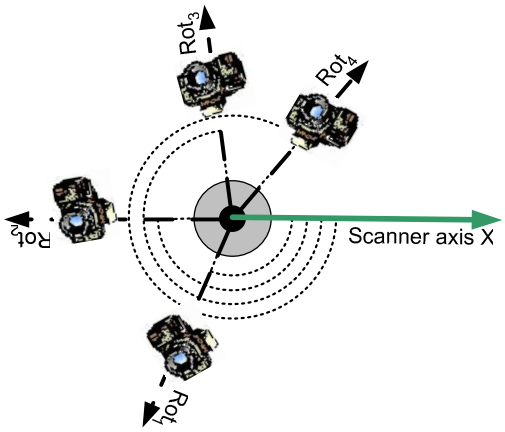

Figure 3: observed rotation for individual camera position

In the calibration of the eccentricity the rotation has to be considered. It is represented in an individual rotation matrix R_{rot_j}. The equation (2) of the radiometric mapping function A_{rad} is upgraded to:

$$X_i = A_{rad}\left(R_{rot_j}, e(T_E, R_E), ior, x', y'\right) \quad (3)$$

With:

R_{rot_j}	Individual rotation matrix

This derived mapping functions show, that the calibration of the radiometric and geometric sensor can also be estimated in this process. Therefore the mapping functions have to be extended with unknown parameters of these sensors additionally. The unknowns are the interior orientation of the radiometric sensor and e.g. correction terms of the measured spherical coordinates and distance of the geometric sensor.

For demonstration the extension of the model is discussed for the unknown interior orientation parameters of the camera. In this connection of calibration task the camera has to stay mounted on top of the scanner. Because of the predictable poor camera configuration in a simultaneous calibration, the difference between single image and multiple image calibration will be shown in a laboratory test.

2.2 Interior orientation

When using a digital camera for photogrammetric tasks, a calibration of the camera has to be done. Fraser (Fraser, 1997) gives an excellent overview of a camera self-calibration model. In a calibration procedure, the parameters for interior and exterior orientation are determined. The interior orientation specifies the characteristic of the camera and is defined by the focal length of the lens, location of the image's principal point and distortion parameters. The exterior orientation describes the spatial relationship between the camera and object. The connection between image and object space is given by the well known collinearity equations (Luhmann, 2003):

$$x - x_0 + \Delta x = -c\frac{r_{11}(X-X_0)+r_{12}(Y-Y_0)+r_{13}(Z-Z_0)}{r_{13}(X-X_0)+r_{23}(Y-Y_0)+r_{33}(Z-Z_0)}$$
$$y - y_0 + \Delta y = -c\frac{r_{21}(X-X_0)+r_{22}(Y-Y_0)+r_{23}(Z-Z_0)}{r_{13}(X-X_0)+r_{23}(Y-Y_0)+r_{33}(Z-Z_0)} \quad (4)$$

The corrections coefficients *Δx and Δy* include parameters modeling the radial symmetric lens distortion and decentering distortion (Brown, 1971). Depending on the camera, also affinity and shear should be considered. The complete correction term is:

$$\Delta x = \Delta x_{rad} + \Delta x_d + \Delta x_{aff}$$
$$\Delta y = \Delta y_{rad} + \Delta y_d + \Delta y_{aff} \quad (5)$$

Thereby the polynomial term of the radial symmetric correction contains the parameters A_1, A_2, A_3, the tangential asymmetric correction is described by B_1, B_2. The x-coordinate is usually also corrected by additional terms for affinity and shear. The terms account the differential scaling between horizontal and vertical pixel spacing and model the non-orthogonality between the x and y axes. Therefore the parameters C_1 and C_2 are used.

Riegl uses in its software RiScan Pro another camera model. It is similar to the one used in the Open Source Computer Vision library (Intel, 2005). Here two potentially different focal lengths (f_x, f_y) are used to cope with different pixel sizes in x and y direction and to correct a cylindrical lens error. Also up to four parameters for the radial distortion can be calculated. The decentering distortion is also modeled. The term for affinity is considered by the different focal lengths, but the shear is not integrated in the model.

The relationship between the three-dimensional object space and two dimensional images is given by:

$$\begin{pmatrix} u' \\ v' \\ w' \end{pmatrix} = \begin{pmatrix} f_x & 0 & c_x \\ 0 & f_y & c_y \\ 0 & 0 & 1 \end{pmatrix} \cdot Rt \cdot \begin{pmatrix} X \\ Y \\ Z \\ W \end{pmatrix} \quad (6)$$

The image coordinates *u'* and *v'* are also corrected by the lens distortion. The parameters describing the distortion are termed as k_1, k_2, k_3 and k_4 for the radial, and p_1, p_2 for tangential correction.

In the following both camera models are used: In the laboratory test the first described model and in the practical test the second model. Anyway we will not distinguish between these models further, because they can be transfered into one another. Since the distortion parameters are highly correlation, it must be considered that always the same parameter set have to be calculated for transformation into each another.

2.3 Laboratory test

As mentioned in the beginning of chapter 2 the differences between single and multiple image calibration with the aspects of reliability and accuracy should be demonstrated. The second goal in this laboratory test is to determine the camera calibration under ideal conditions to acquire reference values for further investigations.

Generally, in case of photogrammetric calibration, the accuracy of the interior orientation estimation depends on:

- The resolution of the image sensor,
- The image scale,
- The accuracy of image points,
- The distribution of control points
- The disposition of taking photographs

The image scale causes the size of mapped control points in image space. The resolution of the sensor defines the scanning frequency of the image signal. The image signal is discretized. One of the basic tasks is the exact determination of the control points in image space. Therefore an interest operator is needed. Interest operators for image point measurement achieve an accuracy of about 0.02 – 0.05 pixels (Luhmann 2003).

Also, a good distribution of control points of the 3D test field is necessary. The image sensor should be covered completely by the mapped points for reliably estimation of distortion.

If the control points of the test field are unknowns a minimum of three images are necessary (Maas, 1998). Also the camera has to be rotated between the positions of taken photographs to minimize correlations of the parameters of the interior orientation.

For the calibration a three dimensional test field with a size of about 1.0 x 1.0 x 0.4 m^3 is used (fig. 4). The control points of the test field are estimated within a bundle adjustment of the multiple image calibration. The lengths of three scale bars are integrated as additional observations. For the taken images an exposure time of 1/80 sec. and an aperture size of 8 are chosen. The mean distance to the object is 1500 mm. The focus of the 14 mm objective is set to infinity. In the laboratory environment similarly light conditions as in possible outdoor applications are realized. For the calculation the software package Australis (Fraser, 2001) and AICON 3D Studio (AICON, 2005) are available.

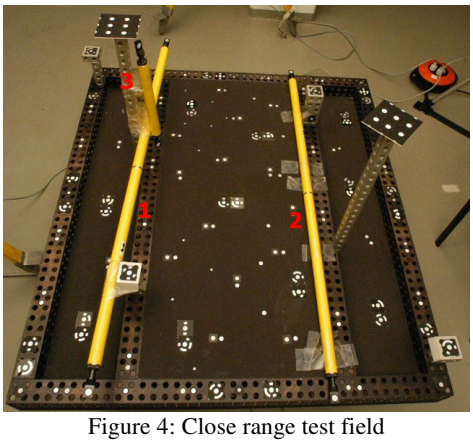

Figure 4: Close range test field

2.3.1 Multiple image calibration

For the multiple image calibration we choose an ideal camera configuration. Totally 16 images are used for the bundle adjustment. The results of the interior orientation are:

parameter	Values [mm]	standard deviation [µm]
C	-13.967	0.299
x_0	-0.264517	0.410
y_0	-0.061695	0.377
A1	-0.00047033	5.561e-004
A2	1.85001e-006	8.692e-006
A3	-2.94623e-009	3.957e-008
B1	-5.60362e-006	5.652e-004
B2	-8.14859e-006	5.179e-004
C1	-2.50556e-005	5.018e-003
C2	-0.000176014	4.961e-003

Table 1: Multi image calibration

2.3.2 Single image calibration

The single image calibration complies with an adjusted resection, where the parameters of the interior orientation are estimated, too. The coordinates of the test field have to be known and are treated as constant. Here, the expansion of the test field in all three dimensions is decisive for the estimation of the camera parameters, because of the correlation between the interior and exterior orientation. To minimize systematic effects and to increase the reliability a large expansion of the test field should be aimed.

The results of the interior orientation are:

parameter	Values [mm]	standard deviation [µm]
C	-13.9629	0.895
x_0	-0.268321	1.199
y_0	-0.0629612	0.889
A1	-0.000468314	1.592e-003
A2	1.81443e-006	2.399e-005
A3	-2.89809e-009	1.045e-007
B1	-1.19962e-005	1.684e-003
B2	-7.49054e-006	1.425e-003
C1	5.10255e-005	1.577e-002
C2	-7.93592e-005	1.485e-002

Table 2: Single image calibration

2.3.3 Comparison of both calibrations

The inner accuracy of the camera constant c and the principal point x_0, y_0 is more than two times higher in the multiple image calibration (tab. 1) than in the single image calibration (tab. 2). The reliability is much worse what is decisive for further application. In the single image calibration the accuracy is directly depending on the accuracy of the control points. Further, there are less control purposes to determine blunders in the control points or image points.

The quality of the estimated distortion parameters is revealed by the coverage and distribution of image points on the sensor.

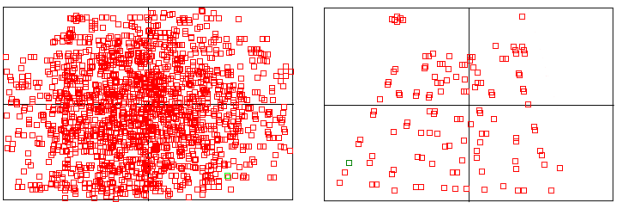

a) Multiple image calibration b) Single image calibration

Figure 5: Comparison of image point distribution

Fig. 5 shows the point distribution on the sensor. In both calibrations the coverage is not perfect. Especially in the image corners points are rare. However, in the multiple image calibration the coverage is more complete than in the single image calibration.

To determine the outer accuracy of both calibrations a comparison in object space is necessary. In this case the three scale bars are used. The lengths of the scale bars are known precisely within a standard deviation of 3 µm. The previously determined control points will be reinserted fixed. The exterior orientation of the images is done with the fixed points of the test field. Now, only the targets of metric scale bars are determined by spatial intersection. The distance deviation between the known length value and the measured one is estimated. This is done with the interior orientation of the multiple image calibration and the single image calibration.

For a more precise statement we let the interior orientation vary within its accuracy and repeat the estimation of the scale bar length. This is done about 100 times. The differences to the three scale bars (cf. fig 4) are shown in chart 1 and 2.

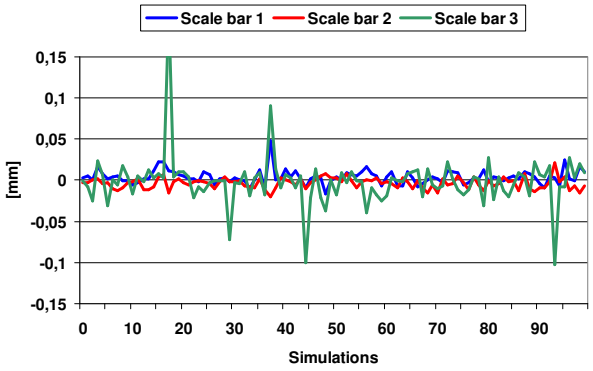

Chart 1: Distance errors of multi image calibration

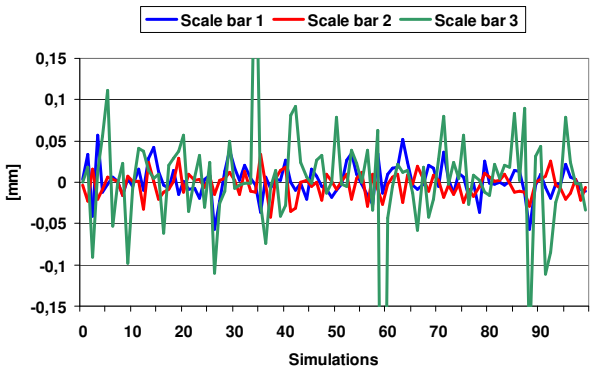

Chart 2: Distance errors of single image calibration

In tab. 3 the results are summarized. Again the accuracy of the multiple image calibration is about three times higher than of the single image calibration. In relation to the first two scale bars the third scale bar (cf. fig. 4) has worse accuracy. That issued from the one sided view of the targets. The bad configuration of image ray intersections implies inaccurate length estimation. This is confirmed by chart 1, where some distances of the vertically installed “scale bar 3” have large variances. In the case of the single image calibration a decreasing accuracy is noticed. Beside the three times worse

standard deviation also the amount of blunder in the estimated distances is increased (cf. chart 2).

	scale bar	Mean deviation [µm]	Standard deviation [µm]
multi image	1	4.070	7.705
	2	-3.476	6.090
	3	-0.532	25.776
single image	1	0.513	22.743
	2	-2.795	15.977
	3	-5.081	87.430

Table 3: Outer accuracy

Contrary to the multiple image calibration the results of the single image calibration are of less quality. Beside the worse accuracy also bad reliability exists. Errors in image point coordinates or control points affect the orientation parameters directly. The parameters of the interior orientation and exterior orientation are highly correlated. Also the coverage of image points on the sensor will be lower.

3. PRACTICAL TEST

For the calibration of the eccentricity between both sensors a three dimensional test field was created in the laboratory hall of the Franzius Institute of the University of Hannover. Therefore 53 retro reflective targets distributed in 3D on the wall and girders of the hall roof serve as control points (fig. 6). The extension of the test field is about 50 m x 20 m x 10 m. The distribution in the depth is excellent, but due to limitations in the accessibility of some parts in the hall, there are some holes in the lateral distribution. Nevertheless, the quantity of the targets provides very good conditions for calibration tasks.

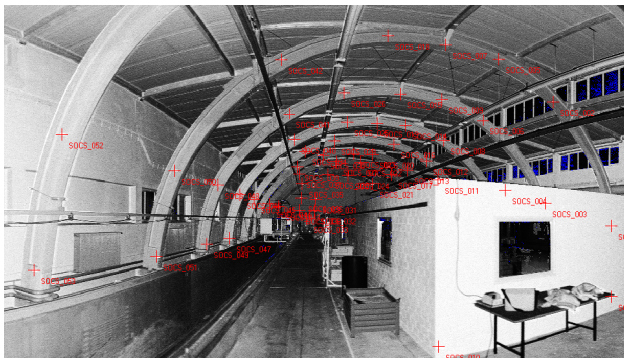

Figure 6: Test field in the Franzius-Hall

For the calibration procedure the hybrid sensor was located in front of the test field. From this position a laser scan is acquired and photographs with the camera are taken in several positions by rotating around the vertical axis of the scanner. Fig. 6 shows the intensity scan of the test field and the distribution of the control points.

For the calculations the software package RiScan Pro (Riegl, 2004) of the scanner manufacture is used. There, operators for the extraction of corresponding points in the scan and the images are provided by the software. In case of the point extraction in the laser scanner data it should be noticed, that in the additionally recorded intensity values the retro reflective targets could be estimated precisely.

For the calibration of the eccentricity, two cases have to be differentiated. First, the interior orientation of the camera and the eccentricity parameters are estimated simultaneously. The software provides a system calibration to estimate both in common. Second, the eccentricity is determined with a constant camera calibration. Object points with known coordinates are identified in at least one acquired image. The correspondences between image and 3D points are established and the eccentricity parameters are calculated by the software.

In this practical test, we carried out both methods to evaluate and demonstrate the differences between them.

3.1 Evaluation of the interior orientation

The estimated interior orientation of the system calibration is compared to the interior orientation of the multiple image calibration of the laboratory test. The results are shown in tab. 4. The values are in pixels. Unfortunately the software provides only little information about the accuracy of the calculated values. The output statistic contains only mean- and max-values of the residuals of the measured image coordinates. Therefore only the parameters are shown.

	System calibration [pix]	**Multiple image calibration [pix]**
$\mathbf{f_x}$	1838.5344	1838.6638
$\mathbf{f_y}$	1838.8774	1838.7242
$\mathbf{c_x}$	1480.9053	1470.0785
$\mathbf{c_y}$	1008.1478	1008.0090
k1	-0.092812228	-0.089029245
k2	0.081201341	0.068981215
k3	-0.020336698	-0.025867248
k4	-0.012959918	0.004787939
p1	-0.000372898	0.000106474
p2	0.000959609	-0.00006248

Table 4: Result of the interior orientation with Riscan Pro

The results of the system calibration show noticeable deviations from the other methods, especially in the principal point. If the parameters are compared with the reference values, the maximum difference of the distorted pixel is about ten pixels in the edge of the sensor. The major reason for this result is obviously the weak geometry of the camera's view points. The difference to the multiple image calibration of the distorted pixels for the whole sensor is shown in chart 3.

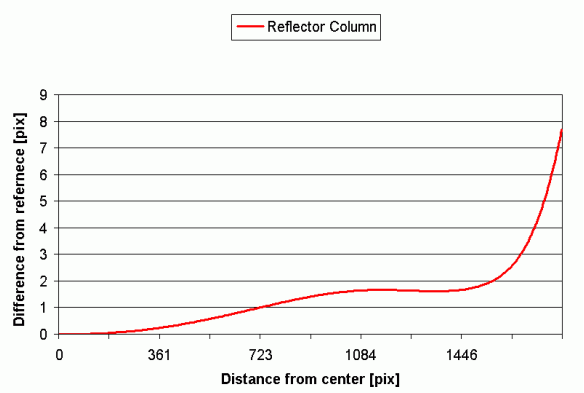

Chart 3: Difference of distortion parameters to the multiple image calibration

3.2 Evaluation of the eccentricity parameters

The results of the eccentricity parameters are listed in tab. 5. Within the system calibration the eccentricity is calibrated with the interior orientation. The three rotations and translations are shown in the first row. Within the second eccentricity calibration the interior orientation of the multiple image calibration is used.

	Rotations			Translations		
	Rot_X [deg]	**Rot_Y [deg]**	**Rot_Z [deg]**	**T_X [m]**	**T_Y [m]**	**T_Z [m]**
with IOR	-1.117	89.934	179.975	-0.220	0.001	-0.090
without IOR	-1.111	90.267	180.001	-0.220	0.000	-0.085
diff.	-0.006	**0.333**	0.026	0.000	-0.001	0.005

Table 5: Results of eccentricity calibration

In tab. 5 also the differences are stated. Due to further analysis we confirm that the differences especially in the rotations will be compensated with the corresponding interior orientation. They are highly correlated.

In case of the interior orientation of the multiple image calibration a better system calibration has to be expected than in case of the common system calibration which complies to the single image calibration.

4. CONCLUSIONS

In this paper we showed how to deal with the calibration of a hybrid laser scanner with a mounted camera. Several calibration methods have been discussed and analyzed, based on a hybrid sensor system from Riegl, The results show, that the calibration of the eccentricity is highly correlated with the interior orientation of the camera. The scanner manufacturer (Riegl, 2004) recommends using the calibration method to estimate the eccentricity and interior orientation in common.

Another aspect of their recommend method is to use a reduced vertical test field in a column that covers the camera's whole vertical field of view and that varies in the depth. Thereby a series of images is taken, each from a different angular position of the camera, by turning the hybrid sensor system automatically. By this procedure a virtual three-dimensional test field is simulated, which covers the complete horizontal and vertical field of view of the camera. The results in this paper pointed out, that within this method in high accuracy applications the interior orientation should not be calibrated. But for the eccentricity estimation it is sufficient and it minimize the cost for test field calibration on the job.

However depending on the postulated accuracy this common calibration could be good enough. It is fast and normally good enough for colorizing 3D point clouds, for instance. Because of the high correlation between the eccentricity and interior orientation, both should be always used in common. For high accuracy applications, the interior orientation should be estimated with multiple image calibration. Only for the calibration of the eccentricity parameters the camera has to be fixed on the scanner.

By further consideration of parameters in the geometric mapping function, possibilities exists to calibrate or to control the laser scanner within the least-squares adjustment of the system calibration.

REFERENCES

AICON, 2005. Product information by AICON 3D Systems GmbH. *http://www.aicon.de/ger/start.htm*, link accessed on January 2005.

Becker, R., Benning, W., Effkemann, C., 2004. 3D-Monoplotting, Kombinierte Auswertung von Laserscannerdaten und photogrammetrischen Aufnahmen. ZFV, 5/2004, pp. 347-355.

Brown, D. C. 1971. Close-Range Camera Calibration. *Photogrammetric Engineering, 37 (8)*, pp. 855-866.

Callidus, 2005. Product information by Callidus GmbH. *http://www.callidus.de/de/cp3200/techn_daten.html*, link accessed on January 2005.

Fraser, Clive S., 1997. Digital camera self-calibration. *ISPRS Journal of Photogrammetry and Remote Sensing*, 52(4), pp. 149-159.

Fraser, Clive S., 2001. Australis User Manual. *Version 5.05*, University of Melbourne.

Intel, 2005. Open Source Computer Vision Library. *http://www.intel.com/research/mrl/research/opencv/*, link accessed January 2005.

iQvolution AG, 2005. Product information by iQvolution AG. *http://www.iqsun.com*, link accessed January 2005.

Leica, 2005. Product information by Leica Geosystems HDS. *http://hds.leica-geosystems.com/products/HDS3000_description.html*, link accessed January 2005.

Luhmann, Th., 2003. Nahbereichsphotogrammetrie. Second Edition, Herbert Wichmann Verlag, Heidelberg.

Maas, H.-G., 1998: Ein Ansatz zur Selbstkalibrierung von Kameras mit instabiler innerer Orientierung. Proceedings of DGPF, Vol. 7, pp.47-53, Munich.

Mensi, 2005. Product information by Mensi Corporation. *http://www.mensi.com/Website2002/gs200.asp*, link accessed January 2005.

Riegl, 2004. RiSCAN PRO Manual. *Version 1.1.1*, Riegl Laser Measurement Systems.

Riegl, 2005. Product information by Riegl LMS GmbH, *http://www.riegl.com/terrestrial_scanners/terrestrial_scanner_overview_/terr_scanner_menu_all.htm*, link accessed January 2005.